Available online at www.sciencedirect.com

SciVerse ScienceDirect

Ceramics International 39 (2013) 5771–5776

CERAMICS INTERNATIONAL

www.elsevier.com/locate/ceramint

Synthesis of hydrophobic ZnO branches by a phase transfer-based solution method

Lanqin Tang[a,b,*], Shaofeng Yang[c], Zichen Wang[b], Bing Zhou[b,1]

[a]College of Chemical and Biological Engineering, Yancheng Institute of Technology, 9 Yingbin Avenue, Yancheng 224051, PR China
[b]College of Chemistry, Jilin University, 2699 Qianjin Street, Changchun 130012, PR China
[c]Department of Chemical and Materials Engineering, University of Alberta, Edmonton, Alberta, Canada T6G 2G6

Received 3 December 2012; accepted 29 December 2012
Available online 11 January 2013

Abstract

ZnO branches with hydrophobic surfaces have been successfully produced in the presence of oleic acid (OA) through a phase transfer-based solution method. Results from field emission scanning electron microscopy, X-ray diffraction analysis and Raman tests revealed that the obtained ZnO particles exhibited well-defined branch-like morphology and hexagonal wurtzite structure. Furthermore, surface characteristics of ZnO could be regulated according to the results of floating and active ratio tests. Fourier transform infrared spectra showed that OA interacted with ZnO particles through strong chemical adsorption. Room-temperature photoluminescence spectra were also used to characterize branch-like ZnO particles. Possible mechanism for the formation and surface modification of branch-shaped ZnO particles was applied.

Keywords: D. ZnO; Powders; Microstructure; Hydrophobic

1. Introduction

Controllable synthesis of ZnO materials was spurred by recent success on the realization of room-temperature ultraviolet lasing from nanorod array [1]. Its great significance for fundamental study of structure–property relations and wide variety of technological potentials have inspired vast research interests, such as catalysts [2–4], sensors [5], photonic crystals [6,7] and others [8,9].

Branch-like ZnO particles exhibited common antibacterial behavior and special super high strength and wear resistance [10,11]. So they were more preferable to be used as functional and structural additives in polymers. However, conventional ZnO particles had high surface polarity, and they usually displayed extremely low stability in organic medium. For these reasons, it was very important to produce branch-like ZnO particles, and simultaneously improve their dispersibility in organic reagents by modifying their surfaces to be hydrophobic. Various efforts were employed to create branch-like ZnO particles. For instance, ZnO branches were fabricated by the oxidation of metallic Zn powder at 550 °C [12]. Zhao et al. [13] have reported the synthesis of branch-shaped ZnO nanostructures by heating the mixture of Zn and Sn powders at 1000 °C for 40 min. Branch-like ZnO particles could be easily produced based on these physical methods. But they were very hard to realize the crystal growth and surface modification of ZnO branches via a facile one-step process. The solution synthesis, because of its simplicity to prepare ZnO particles at a relatively low temperature, has attracted more interests. Recently, many efforts have been concentrated on the synthesis of ZnO branches via the solution-based method [14–19]. For example, ZnO branches were produced by a citric acid-assisted hydrothermal process [14]. In that work, citrates attaching on $ZnO/Zn(OH)_2$ intermediate acted as a kind of hard template for the formation of regular branch-like ZnO particles. Besides, by tuning the molar ratios of sodium

*Corresponding author at: College of Chemical and Biological Engineering, Yancheng Institute of Technology, 9 Yingbin Avenue, Yancheng 224051, PR China. Tel./fax: +86 515 8829 8615.
[1]Tel./fax: +86 515 8829 8615.
E-mail addresses: lanqin_tang@ycit.edu.cn (L. Tang), zhoubing@jlu.edu.cn (B. Zhou).

0272-8842/$ - see front matter © 2013 Elsevier Ltd and Techna Group S.r.l. All rights reserved.
http://dx.doi.org/10.1016/j.ceramint.2012.12.096

hydroxide to zinc acetate in a hydrothermal phase, controlled branch-like ZnO particles were obtained [16]. Similar works were also reported that ZnO branches were preferred to be formed at higher solution pH (>7.0) [17–19]. However, the fabrication of ZnO branches with hydrophobic surfaces was rarely reported through the facile one-step process.

In this paper, hydrophobic ZnO branches are produced through a phase transfer-based solution method. This method has its special advantages: (1) the formation and surface modification of ZnO branches are realized by a facile one-step process; and (2) ZnO branches show perfect compatibility with common organic reagents. The mechanism for the formation of branch-like ZnO particles with hydrophobic surfaces has been presented.

2. Experimental section

2.1. Preparation

ZnO particles were produced according to the work reported by Zhang and Li [20]. In a typical synthesis of hydrophobic ZnO branches, 0.24 g OA (about 3.0 wt% of ZnO) was added into 100 mL of 1.0 M Na_2CO_3 solution, vigorously stirred for 5 min, and heated to 70 °C. Then, a solution of 100 mL $ZnSO_4$ (1.0 M) was dropped. Subsequently, a solution of 100 mL NaOH (1.1 M) was added drop-wise resulting in a white slurry, which was then maintained at 70 °C for 3 h. Obtained sample was denoted as sample-A. Contrast experiment was also conducted in the absence of OA, and obtained sample was denoted as sample-A_0.

2.2. Characterization

The products obtained from the whole formation process were monitored by field emission scanning electron microscope (FESEM) observations (JEOL JSM-6700F) with an acceleration voltage of 5.0 kV. The crystal structures of ZnO samples were examined by X-ray diffraction (XRD), using a Rigaku D/Max-RA Cu Kα diffractometer at a scan rate of $6^\circ/min^{-1}$. The KBr pellet method was used to record FT-IR spectra of samples in the range of 400–4000 cm^{-1} (Nicolet Bruker FT 5DX). Contact angles were measured by the sessile drop method using a conventional drop shape technique OCA 20 apparatus (DataPhysics Instrument GmbH, Filderstadt, Germany). In this paper, the measurements were started as fast as possible when the drop had been formed on the tip of a micro-syringe, which was gently deposited on the substrate to ensure that a Cassie drop was formed. The distance between the syringe and the solid surface was kept constant throughout the series of measurement. Raman spectra were recorded using a Renishaw 1000 Raman microscope with a 514.5 nm Ar^+ laser as an excitation source. Room-temperature photoluminescence spectra (PL) were achieved on an Edinbergh instrument FLS 920 using a 310 nm excitation line.

3. Results and discussion

3.1. Surface property of ZnO particles

Effects of the amount of OA on surface properties of produced ZnO samples are roughly analyzed by floating tests. The ratio of the floated product to the overall weight of the sample and the weight ratio of OA to ZnO are expressed as R and W, respectively. Therefore, high R shows good hydrophobicity of ZnO particles. Table 1 shows the corresponding results when different amounts of OA are used. It can be seen that R of above 90.0% can be achieved by increasing W to 2.0 wt%. Besides, when W is 3.0 wt%, R will increase to 99.0%. Therefore, in order to obtain ZnO branches with excellent hydrophobic surfaces, weight ratio of OA to ZnO is optimized to be 3.0 wt%.

Sample-A and sample-A_0 are analyzed by floating and contact angle tests to study their surface characteristics. In order to conduct the floating tests, 0.05 g ZnO powder is added into a tube with 12 mL water, sealed and oscillated vigorously for several times from top to bottom. As Fig. 1a1 shows, phase separation phenomenon is obviously detected and sample-A is floating on the surface of water; while Fig. 1a2 shows that sample-A_0 is uniformly dispersed in

Table 1
Effects of the amount of OA on surface properties of ZnO samples.

W (wt%)	R (%)
0.5	28.0
1.0	52.0
2.0	93.0
3.0	99.0

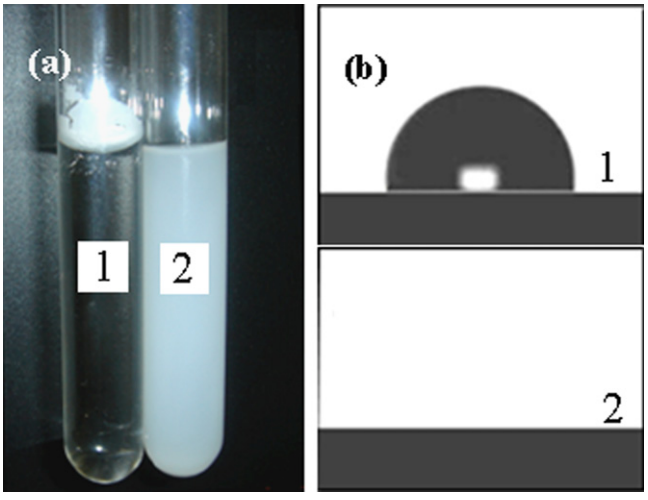

Fig. 1. Images of samples-A (a1) and -A_0 (a2) in distilled water and water contact angles of samples-A (b1) and -A_0 (b2) obtained in the presence and absence of oleic acid (OA), respectively.

water. Further contact angle test is conducted according to our previous work [21]. As Fig. 1b1 shows, a drip with a contact angle of about 102° is observed. No stable drip is formed on the surface of sample-A_0 (Fig. 1b2). Therefore, ZnO particles with hydrophobic surfaces are successfully fabricated through the simple solution-based method.

To study the dispersibility of sample-A in organic reagents at room temperature, two types of common organic reagents are chosen, including ethylene glycol and cyclohexane. From Fig. 2 it can be seen that, particles from sample-A are uniformly dispersed in these organic reagents and show perfect compatibility with them, which is quite different from those shown in Fig. 1a1. Therefore, ZnO particles obtained in the presence of OA could be expected to be applied in these systems, to study their special properties.

3.2. Structure and morphology

Fig. 3 shows the X-ray diffraction patterns of sample-A and sample-A_0. All these X-ray diffraction peaks can be indexed as hexagonal wurtzite structure (space group *P*63*mc*), which are consistent with the values in the standard card (JCPDS 36-1451). Compared with the peaks shown in Fig. 3a, the modification process leads to stronger diffraction peaks (Fig. 3b), which seem to indicate the effect of OA on the growth of ZnO crystallite. Even if fabricated at a low temperature (70 °C), ZnO nanostructures crystallize well, basing on the intensity and half width of the XRD patterns. Furthermore, the texture coefficient values of sample-A and sample-A_0 are calculated according

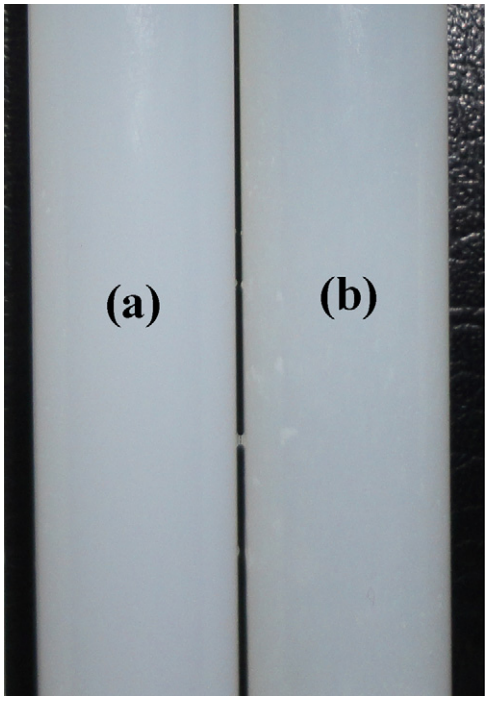

Fig. 2. Pictures of oleic acid (OA) modified sample-A in ethylene glycol (a) and cyclohexane (b).

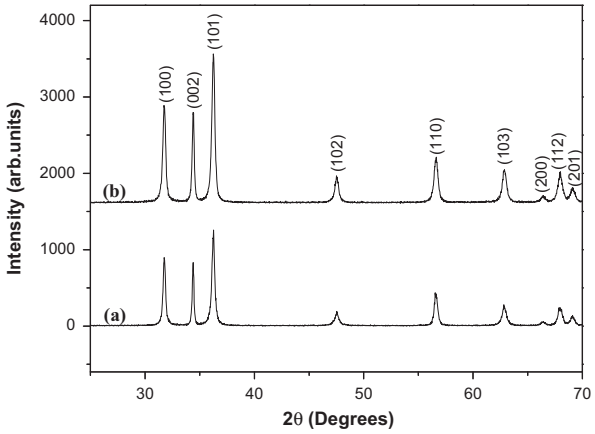

Fig. 3. X-ray diffraction patterns of sample-A_0 (a) and sample-A (b) obtained in the absence and presence of oleic acid (OA), respectively.

Table 2
Texture coefficient of sample-A and sample-A_0.

Sample	Texture coefficient		
	$T_{c(100)}$	$T_{c(002)}$	$T_{c(101)}$
A_0	0.99	1.20	0.80
A	0.98	1.17	0.85

to their three main corresponding X-ray diffraction peaks (Table 2). Both the texture coefficient of (002) face are stronger than the (100) and (101) orientations. A sample with randomly oriented crystallites presents a $Tc_{(hkl)}$ of 1, while a larger value indicates an abundance of crystallites oriented to the (*hkl*) plane [22]. These results indicate that sample-A and sample-A_0 are both oriented in the $<002>$ direction.

Fig. 4 illustrates the FESEM micrographs of sample-A and sample-A_0. As Fig. 4a shows, the obtained ZnO particles exhibit well-defined branch-like morphology. The average size of branches is about 2.0 μm, and a branch length is about 1.0 μm. From the high-magnification image shown in Fig. 4b, it can be seen that number of the petals of a branch is usually six. Different number of branches will lead to excellent properties of ZnO, such as ethanol sensors, photocatalysis [10,23]. The FESEM image of sample-A_0 shows that ZnO rods and incomplete branches are produced in the absence of OA (Fig. 4c). It shows that OA plays an important role in the formation of these special ZnO branches.

3.3. Mechanism

To study the mechanism of the special surface properties, sample-A is purified by soxhlet extraction with distilled water for 12 h, and then analyzed by FT-IR tests. Fig. 5 shows the FT-IR spectra of pure ZnO (a), OA (b), and purified sample-A (c). Among them, Fig. 5a shows the standard pattern with

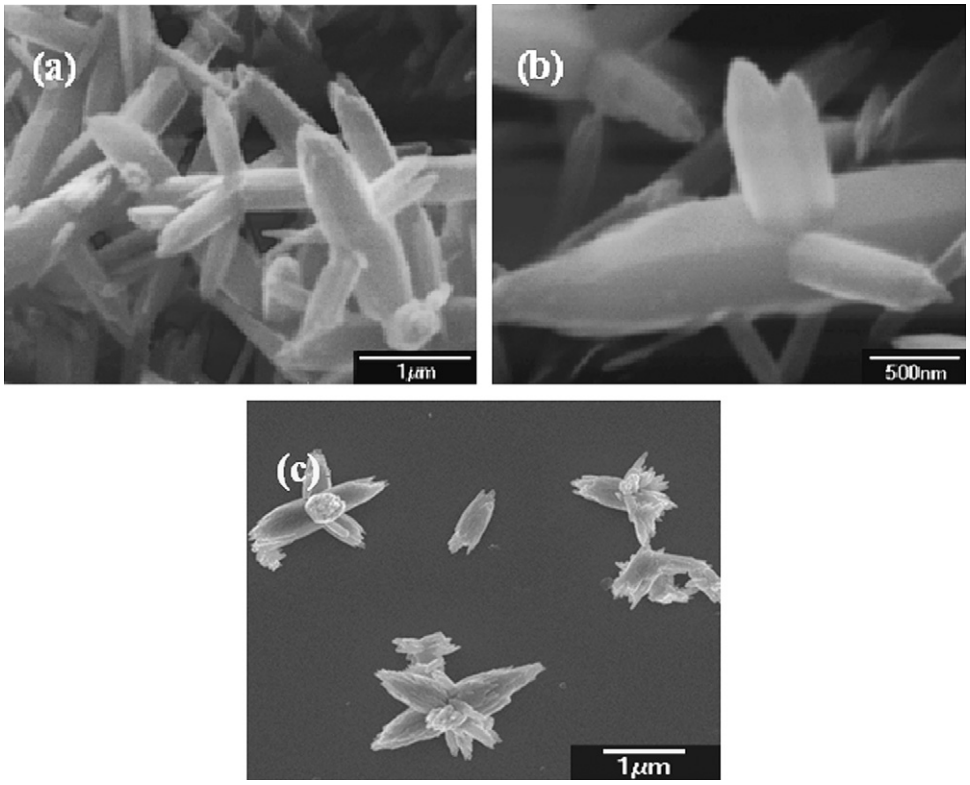

Fig. 4. FESEM images of sample-A (a, b) and sample-A_0 (c) obtained in the presence and absence of oleic acid (OA), respectively.

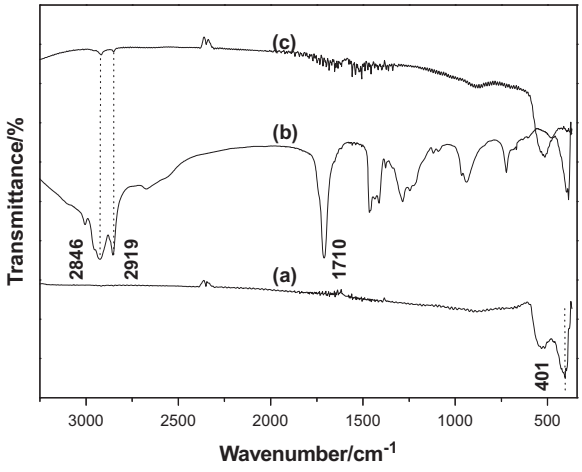

Fig. 5. FT-IR spectra of pure ZnO (a), oleic acid (OA, b) and purified sample-A (c).

the characteristic FT-IR absorption band of ZnO at about 401 cm^{-1}. Adsorption peak at 1710 cm^{-1} is attributed to carbonyl stretching vibration from OA, and peaks around 2916 and 2846 cm^{-1} ($\nu(CH_2)$) are consistent with the appearance of the alkyl groups from OA. From Fig. 5c, peaks attributed to alkyl groups are found. It is convinced that a strong chemical bond exists between OA and ZnO surfaces [21].

In order to monitor the morphology evolvement of the whole process, time-dependent experiments are performed. Fig. 6 shows the FE–SEM images of ZnO samples-B, and -C obtained by regular sampling (15 min and 1 h respectively). When the reaction time is 15 min, rods with "active sites" are detected (arrows indicated parts, sample-B, Fig. 6a). Among the works about the production of branch-like ZnO particles [14–19], this special kind of rods is rarely reported. When reaction time is increased to 1 h, subsequent growth of rods from these "active sites" is detected in sample-C (indicated by an arrow, Fig. 6b).

Based on the above analyses, a possible mechanism could be described below. In principle, when the area of *c*-face in the particle becomes larger than the critical size for island nucleation, further nucleation occurs on it and the process repeats to form rod-like ZnO structures [24]. While in the presence of OA, surface property of obtained ZnO particles will be tailored by chemical adsorption of them (Figs. 1 and 5). According to Fig. 6, many "active sites" are generated on the surfaces of these ZnO rods [25]. To match the crystals, continuative growth and re-mineralization of rods are induced from these active sites. Therefore, oriented epitaxial growth as well as surface functionalization of ZnO branches can be realized at the same time. Furthermore, intermediate will lead to the formation of rods with "active sites" and eventually the formation of branches. These results show that the influential factors on the morphology of ZnO are derived from the comprehensive effects of intermediates and OA, not simply the additive itself.

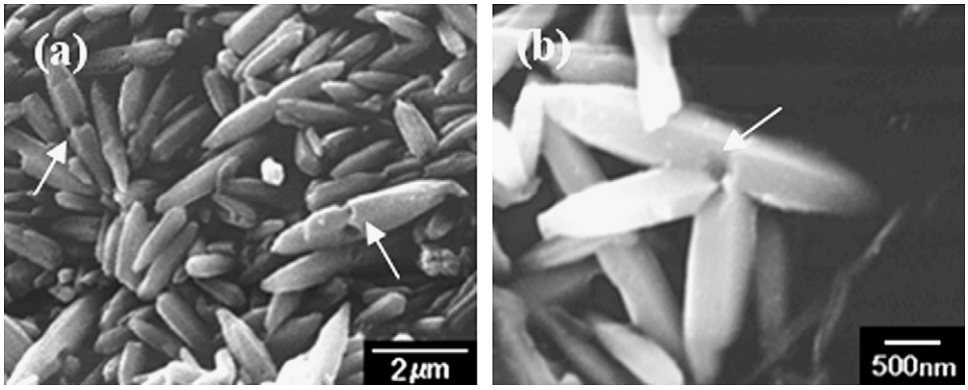

Fig. 6. FESEM images of ZnO particles obtained in the presence of oleic acid (OA) for 15 min and 1 h.

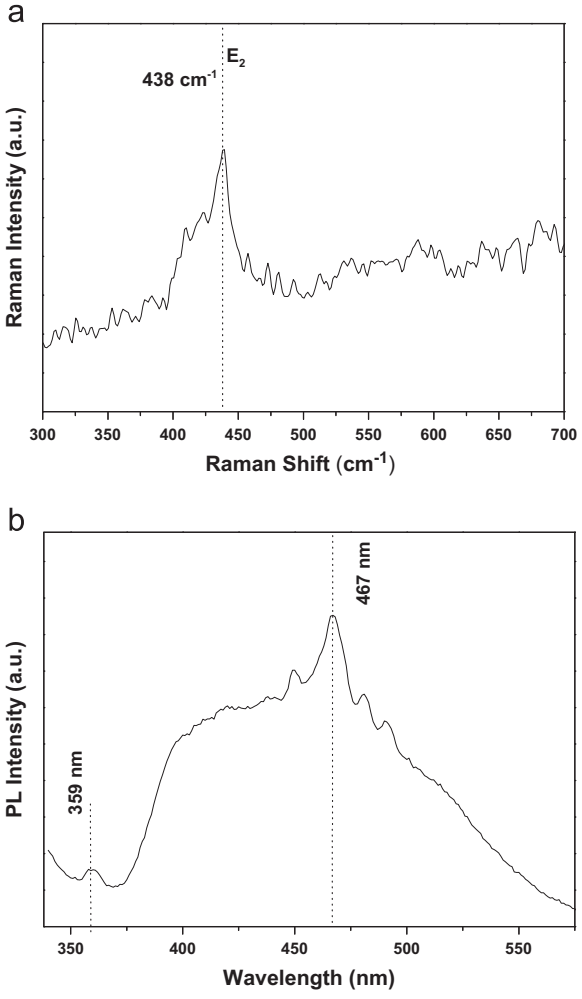

Fig. 7. Raman (a) and PL (b) spectra of sample-A obtained in the presence of oleic acid (OA).

3.4. Optical properties

Raman spectroscopy is based on the Raman effect, which is the inelastic scattering of photons by molecules. Optical phonons at the Γ point of the Brillouin zone have the following irreducible representation:

$$\Gamma_{\mathrm{opt}} = 1A_1 + 2B_1 + 1E_1 + 2E_2,$$

where polar A_1 and E_1 modes split into transverse (TO) and longitudinal optical (LO) phonons and they are all Raman and infrared active. The nonpolar E_2 modes are Raman active only and the B_1 modes are Raman inactive. Raman spectra of sample-A are shown in Fig. 7a. Raman peak at 438 cm^{-1} is the characteristic band of wurtzite phase involving the oxygen motion, and is corresponding to the nonpolar optical phonon E_2 mode. Room-temperature PL measurement of sample-A is further characterized. As Fig. 7b shows, both UV and green emissions locating at 359 nm and 467 nm are obviously detected, which are attributed to the radiative annihilation of excitons, and the recombination of electrons in singly occupied oxygen vacancies with photo excited holes, respectively [26].

4. Conclusion

ZnO branches with hydrophobic surface properties were fabricated through a facile phase transfer-based solution method. On the basis of FESEM, FT-IR, and active ratio observations, OA played an important role in promoting the formation of rod-like branches and at the same time realizing the surface functionalization of produced ZnO samples. This route enhanced the influences of modifiers and intermediates on the morphologies of obtained ZnO products, which could be applied to the synthesis of other oxides like copper oxide. Furthermore, the obtained branch-like ZnO samples possessed an obvious UV emission at about 359 nm.

Acknowledgment

This work was supported by the Talents Introduction Project of Yancheng Institute of Technology (XKR2011008) and the Key Laboratory for Advanced Technology in Environmental Protection of Jiangsu Province (AE201122 and AE201165).

References

[1] M.H. Huang, S. Mao, H. Feick, H.Q. Yan, Y.Y. Wu, H. Kind, R. Russo, P.D. Yang, Room-temperature ultraviolet nanowire nanolasers, Science 292 (2001) 1897–1899.

[2] P.C.K. Vesborg, I. Chorkendorff, I. Knudsen, O. Balmes, J. Nerlov, A.M. Molenbroek, B.S. Clausen, S. Helveg, Transient behavior of Cu/ZnO-based methanol synthesis catalysts, Journal of Catalysis 262 (2009) 65–72.

[3] M. Chambon, S. Abanades, G. Flamant, Solar thermal reduction of ZnO and SnO_2: characterization of the recombination reaction with O_2, Chemical Engineering Science 65 (2010) 3671–3680.

[4] S. Sá, J.M. Sousa, A. Mendes, Steam reforming of methanol over a $CuO/ZnO/Al_2O_3$ catalyst part II: a carbon membrane reactor, Chemical Engineering Science 66 (2011) 5523–5530.

[5] D. Calestani, M. Zha, R. Mosca, A. Zappettini, M.C. Carotta, V.D. Natale, L. Zanotti, Growth of ZnO tetrapods for nanostructure-based gas sensors, Sensors and Actuators B: Chemical 144 (2010) 472–478.

[6] S.M. Abrarov, R.M. Abrarov, Broadening of band-gap in photonic crystals with optically saturated media, Optics Communications 281 (2008) 3131–3136.

[7] M.A. Mastro, L. Mazeina, B.J. Kim, S.M. Prokes, J. Hite, C.R. Eddy, J. Kim, Vertical zinc oxide nanowires embedded in self-assembled photonic crystal, Photonics and Nanostructers 9 (2011) 91–94.

[8] C.L. Kuo, C.L. Wang, H.H. Ko, W.S. Hwang, K.M. Chang, W.L. Li, H.H. Huang, Y.H. Chang, M.C. Wang, Synthesis of zinc oxide nanocrystalline powders for cosmetic applications, Ceramics International 36 (2010) 693–698.

[9] M. Peiteado, Y. Iglesias, A.C. Caballero, Sodium impurities in ZnO–Bi_2O_3–Sb_2O_3 based varistors, Ceramics International 37 (2011) 819–824.

[10] X.Y. Ma, W.D. Zhang, Effects of flower-like ZnO nanowhiskers on the mechanical, thermal and antibacterial properties of waterborne polyurethane, Polymer Degradation and Stability 94 (2009) 1103–1109.

[11] S.B. Wang, S.R. Ge, D.K. Zhang, Comparison of tribological behavior of nylon composites filled with zinc oxide particles and whiskers, Wear 266 (2009) 248–254.

[12] X.H. Sun, S. Lam, T.K. Sham, F. Heigl, A. Ju1rgensen, N.B. Wong, Synthesis and synchrotron light-induced luminescence of ZnO nanostructures: nanowires, nanoneedles, nanoflowers, and tubular whiskers, Journal of Physical Chemistry B 109 (2005) 3120–3125.

[13] J.W. Zhao, L.R. Qin, Z.D. Xiao, L.D. Zhang, Synthesis and characterization of novel flower-shaped ZnO nanostructures, Materials Chemistry and Physics 105 (2007) 194–198.

[14] Y.J. Sun, Y. Lu, Y. Yu, X.G. Kong, Q.H. Zeng, Y.L. Zhang, H. Zhang, Template-assemble synthesis of ZnO:Er nanostructure and their upconversion luminescence properties, Journal of Nanoscience and Nanotechnology 9 (2009) 1316–1320.

[15] Y.L. Lai, M. Meng, Y.F. Yu, X.T. Wang, T. Ding, Photoluminescence and photocatalysis of the flower-like nano-ZnO photocatalysts prepared by a facile hydrothermal method with or without ultrasonic assistance, Applied Catalysis B 105 (2011) 335–345.

[16] Y.Y. Zhang, J. Mu, Controllable synthesis of flower- and rod-like ZnO nanostructures by simply tuning the ratio of sodium hydroxide to zinc acetate, Nanotechnology 18 (2007) 075606.

[17] W. Huang, J.G. Jia, X.W. Zhou, Y. Lin, Morphology controllable synthesis of ZnO crystals-pH-dependent growth, Materials Chemistry and Physics 123 (2010) 104–108.

[18] M.V. Vaishampayan, I.S. Mulla, S.S. Joshi, Low temperature pH dependent synthesis of flower-like ZnO nanostructures with enhanced photocatalytic activity, Materials Research Bulletin 46 (2010) 771–778.

[19] W.Y. Wu, W.Y. Kung, J.M. Ting, Effect of pH values on the morphology of zinc oxide nanostructures and their photoluminescence spectra, Journal of the American Ceramic Society 94 (2011) 699–703.

[20] S.C. Zhang, X.G. Li, Preparation of ZnO particles by precipitation transformation method and its inherent formation mechanisms, Colloids and Surfaces A: Physicochemical and Engineering Aspects 226 (2003) 35–44.

[21] L.Q. Tang, B. Zhou, Y.M. Tian, F. Sun, Y.L. Li, Z.C. Wang, Synthesis and surface hydrophobic functionalization of ZnO nanocrystals via a facile one-step solution method, Chemical Engineering Journal 139 (2008) 642–648.

[22] R. Romero, D. Leinen, E.A. Dalchiele, J.R. Ramos-Barrado, F. Martín, The effects of zinc acetate and zinc chloride precursors on the preferred crystalline orientation of ZnO and Al-doped ZnO thin films obtained by spray pyrolysis, Thin Solid Films 515 (2006) 1942–1949.

[23] Z.R. Tian, J.A. Voigt, J. Liu, B. Mckenzie, M.J. Mcdermott, M.A. Rodriguez, H. Konishi, H.F. Xu, Complex and oriented ZnO nanostructures, Nature Materials 2 (2003) 821–826.

[24] J. Tersoff, A.W.D. Vandergon, R.M. Tromp, Critical island size for layer-by-layer growth, Physical Review Letters 72 (1994) 266–269.

[25] C. Pacholski, A. Kornowski, H. Weller, Self-assembly of ZnO: from nanodots to nanorods, Angewandte Chemie, International Edition 41 (2002) 1188–1191.

[26] S. Monticone, R. Tufeu, A.V. Kanaev, UV and visible fluorescence of colloidal ZnO nanoparticles, Journal of Physical Chemistry B 102 (1998) 2854–2862.